We are IntechOpen, the world's leading publisher of Open Access books Built by scientists, for scientists

4,800
Open access books available

122,000
International authors and editors

135M
Downloads

Our authors are among the

154
Countries delivered to

TOP 1%
most cited scientists

12.2%
Contributors from top 500 universities

WEB OF SCIENCE™

Selection of our books indexed in the Book Citation Index in Web of Science™ Core Collection (BKCI)

Interested in publishing with us?
Contact book.department@intechopen.com

Numbers displayed above are based on latest data collected.
For more information visit www.intechopen.com

15

Molecular Imaging in TB: From the Bench to the Clinic

Nuria Andreu[1], Paul T. Elkington[1] and Siouxsie Wiles[1,2]
[1]*Imperial College London,*
[2]*University of Auckland,*
[1]*United Kingdom*
[2]*New Zealand*

1. Introduction

Despite all efforts, tuberculosis (TB) still constitutes a serious global health threat with 9.4 million new cases and 1.7 million deaths worldwide in 2009 (World Health Organisation, 2010). Furthermore, an estimated one third of the worlds' population is infected with the bacterium responsible, *Mycobacterium tuberculosis*. The main handicaps in fighting TB include a vaccine which works poorly in the most affected populations, and an arduous treatment regimen, involving a combination of several drugs taken over many months. This is further complicated by the emergence of multi-drug resistant (MDR) and extensively drug-resistant (XDR) *M. tuberculosis* strains, which require even longer treatment times with less well-tolerated drugs. Eradication of TB will require the development of new drugs and vaccines, alongside improved methods for diagnosis and monitoring treatment efficacy. With the vast burden of disease falling in resource poor settings, the challenge will also be to develop methodologies that can be deployed with minimal investment in infrastructure, maintenance and staff expertise.

Recent decades have seen the emergence of the new discipline of molecular imaging. In essence, molecular imaging enables the non-invasive visualisation, characterisation, and quantification of biological processes taking place within intact living subjects, be it a mouse or man (Filippi & Rocca, 2011; Horky & Treves, 2011; Pysz et al., 2010; Sandhu et al., 2010). Imaging has long been applied to managing TB; simple chest x-rays have allowed clinicians to visualise TB in people for over a century (Singh & Nath, 1994). However, the new molecular imaging techniques are revolutionising medical research, with the potential to translate into significant changes in clinical practice. In this chapter we describe the new generation of imaging modalities and how these are being applied to eradicating TB, from the laboratory bench and in to the clinic.

2. Molecular imaging modalities

Molecular imaging is broadly defined as the visualisation, characterisation and quantification of biological processes, at the cellular and subcellular level, within living subjects. Importantly, the non-invasive nature of the techniques enables the study of disease

processes longitudinally within the same subjects, a powerful tool indeed for elucidating host-pathogen interactions and treatment efficacy. A number of imaging modalities have emerged, which vary in their methods of image generation, spatial resolution, depth penetration and detection thresholds (Table 1). As a result each modality has different advantages and disadvantages (Table 2), suggesting the techniques should be used to complement each other to answer specific research questions.

Modality	Image generation	Spatial resolution	Depth penetration
Computed tomography (CT)	x-rays	50-200 μm	No limit
Magnetic resonance imaging (MRI)	Radiowaves	25-100 μm	No limit
Positron emission tomography (PET)	High energy γ-rays	1-2 mm	No limit
Single photon emission (SPE) CT	Lower energy γ-rays	1-2 mm	No limit
Optical	Visible light	2-5 mm	1-2 cm

Table 1. Features of currently employed imaging modalities (Adapted from Massoud & Gambhir, 2003)

2.1 Computed Tomography (CT)

CT imaging combines low-dose x-rays and computing to produce reconstructions of the internal organs and tissues. This is possible because diverse tissue types differentially absorb x-rays as they pass through the body. CT is not a molecular imaging tool per se, but can provide important information on anatomical changes which arise as a result of disease processes. Widely used in clinical settings, there are now a number of miniaturised machines suitable for scanning of small animals (often referred to as micro-CT). To collect data, the subject is placed on a motorised table, which then moves into the lead-encased CT machine. Inside, an x-ray source and a set of x-ray detectors rotate 360 degrees around the subject in synchrony. At every angle, the detectors record the x-rays passing through the subject to provide a digital projection which is collected and sent to a computer. The x-ray source produces a narrow, fan-shaped beam, with widths ranging from 1 to 20 mm. In axial CT, which is commonly used for head scans, the table is stationary during a rotation, after which it is moved along for the next slice. In helical CT, which is commonly used for body scans, the table moves continuously as the x-ray source and detectors rotate, producing a spiral or helical scan. Clinical machines typically have multiple rows of detectors operating side by side, so that many slices (currently up to 64) can be imaged simultaneously, reducing the overall scanning time. As an alternative to the fan-shaped x-ray beam, small animal scanners may instead use a cone-shaped beam, where the scanned subject is captured completely in one rotation, speeding up the imaging process. The data are processed by computer to produce a series of image slices representing two-dimensional (2D) or three-dimensional (3D) views of the target organ or body region.

Modality	Advantages	Disadvantages
CT	Unlimited depth penetration High spatial resolution Whole body imaging of animals and humans Short aquisition times (minutes) Anatomical imaging	Radiation exposure Poor soft tissue contrast Moderately expensive
MRI	Unlimited depth penetration High spatial resolution Whole body imaging of animals and humans Good soft tissue contrast Non-ionising radiation Anatomical imaging	Expensive Long acquisition times (minutes to hours) Limited sensitivity
PET	Unlimited depth penetration Whole body imaging of animals and humans Can be combined with CT for anatomical imaging	Radiation exposure Expensive Long acquisition times (minutes to hours) Low spatial resolution PET cyclotron or generator needed
SPECT	Unlimited depth penetration Whole body imaging of animals and humans Can be combined with CT for anatomical imaging Can distinguish between radionuclides, so multiple processes can be imaged simultaneously	Radiation exposure Long acquisition times (minutes to hours) Low spatial resolution
Optical	Short aquisition times Highly sensitive and quantitative Whole body imaging of animals Can be combined with CT for anatomical imaging of animals Inexpensive	Limited depth penetration Whole body imaging of humans not possible

Table 2. Advantages and disadvantages of imaging modalities (Adapted from Massoud & Gambhir, 2003)

The spatial resolution of CT is primarily limited by scanning times, the size of the x-ray source, and the sensitivity of the detection system. In addition, CT has relatively poor soft tissue contrast; generally, iodinated molecules are applied as contrast agents, owing to the high x-ray absorption coefficient of iodine (McClennan, 1994). Current iodine-based contrast agents have several limitations, including adverse reactions, renal toxicity, vascular permeation and rapid renal clearance resulting in limited imaging times. As a result, alternative contrast agents have been suggested, such as polymer-coated Bi_2S_3 (Rabin et al., 2006) or gold nanoparticles (Hainfield et al., 2006). Indeed, gadolinium chelate-coated gold nanoparticles have been reported as dual imaging probes for CT and magnetic resonance

imaging (MRI) (Alric et al, 2008). Tissue contrast can also be improved by using a dual-energy x-ray method in which the projection data are acquired using two different x-ray spectra (Taschereau et al., 2010). However, one of the major limitations of CT is radiation exposure, and while the doses are low, they are not negligible and this can limit repeated imaging of the subject.

2.2 Magnetic Resonance Imaging (MRI)

MRI is based on the interactions of atoms and molecules in a tissue of interest, upon exposure to a magnetic field. In addition to providing detailed structural images, MRI can obtain physiological information through the use of specific contrast agents. While the proton ^{1}H is most widely used in MRI, due to the abundance of water within soft tissues, other paramagnetic atoms such as ^{13}C, ^{17}O, ^{19}F, ^{23}Na and ^{31}P are also useful. Within an MRI scanner, a strong 'coiled' magnet produces a magnetic field with a gradient in the X, Y and Z directions, which causes nuclei to align themselves. The device also contains a radiofrequency (RF) coil which is used to produce a temporary RF pulse, resulting in a change in nuclei alignment. Following the pulse, the protons return to their baseline orientation (known as relaxation) which is detected as a change in electromagnetic flux.

The behaviour of the energy inserted into the system is described by two relaxation constants: the longitudinal relaxation time (T1) or the transverse relaxation time (T2). Different tissues have different relaxation times and this can be used to produce endogenous contrast between different tissues. Addition of exogenous contrast agents can further enhance tissue contrast by selectively shortening either T1 or T2 in a tissue of interest. According to their magnetic properties, contrast agents can be classified as paramagnetic (for example, gadolinium based agents) or superparamagnetic (for example, iron oxide nanoparticles) (reviewed in Geraldes & Laurent, 2009). Depending on their biodistribution patterns, different contrast agents can also be utilised to image specific anatomical regions. MRI is becoming widely used in both clinical and preclinical settings, with dedicated MRI machines available for humans and rodents. An advantage of MRI is that it does not involve ionising radiation, has unlimited depth penetration and good soft tissue contrast. However, it is expensive and scanning times are typically long, from minutes to hours.

2.3 Positron Emission Tomography (PET)

PET imaging involves the visualisation of a radiotracer, a biomarker labelled with a positron emitter. The positron emitters typically used are isotopes with short half-lives (several hours to a few minutes), such as ^{11}C, ^{13}N, ^{15}On and ^{18}F. Radiotracers are typically made to reflect compounds normally used by the body, such as glucose or ammonia, or molecules that bind to specific receptors. Once the radiotracer is injected into a subject, it therefore distributes based on its similarity to the original biomarker compound. The most commonly used radiotracer is an analogue of glucose labelled with ^{18}F, [^{18}F]-2-fluoro-deoxy-D-glucose, ([^{18}F]-FDG). A major advantage of PET imaging is that it can be used to trace the fate of any compound, provided it can be radiolabeled with a PET isotope. As a result, the processes that can be probed using PET imaging are virtually limitless, and radiotracers for new target molecules and processes continue to be developed. For a summary of available PET radiotracers see Pysz et al., 2010. Dedicated clinical and small animal PET scanners are now available.

PET imaging is based on the fact that the incorporated radionucleotide undergoes positive β decay and emits a positron. The positron travels a few mm before it annihilates with an electron to emit a pair of photons moving in approximately opposite directions. These photons are then detected by the scanning device. As the photons are travelling at approximately 180° to each other, it is possible to localise their source along a straight line of coincidence known as a line of response (LOR). The distribution pattern of the LORs is then used to reconstruct an image of the radioactivity distribution within the subject. One minor limitation of utilising photons is that they are differentially attenuated as they traverse different thicknesses of tissue. This attenuation results in the reconstruction of structures deep within the body as having falsely low uptake of the radiotracer. However this attenuation can be corrected for by combining PET with CT imaging.

Despite the great promise of PET imaging, there are a number of significant disadvantages. One is the use of ionising radiation, although this is minimised by the use of radioisotopes with short half-lives. However, these short half-lives require both costly cyclotron generators and chemical synthesis apparatus within close proximity to the scanning facility for the production of the radiotracers. This certainly limits the use of the technology within resource poor settings. Furthermore, scanning times are typically long, from minutes to hours, and the technique provides low spatial resolution.

2.4 Single Photon Emission Computed Tomography (SPECT)

Like PET, SPECT imaging is based on the distribution and uptake of a radiolabelled tracer after injection into a subject. Unlike PET tracers, SPECT radionucleotides undergo radioactive decay and emit γ-rays of a particular energy, which are then captured by an external detector. A number of 2D projections are captured from multiple angles which, when combined, form a 3D image. Radiotracers based upon radioactive metals, such as ^{111}In, ^{188}Re, ^{131}I, and ^{133}Xe, are often used. For a summary of available SPECT radiotracers see Pysz et al., 2010. PET and SPECT imaging share many of the same advantages and disadvantages. However, while PET is more sensitive, SPECT imaging is much cheaper largely thanks to the availability of different radiotracers which are longer lived and easier to obtain. Moreover, different SPECT radiotracers have different energies enabling multiple tracers to be used to image different processes.

2.5 Optical Imaging

The electromagnetic radiation we refer to as light undergoes a range of interactions when propagating through tissue. Importantly, these interactions depend on the structural arrangement and physical properties of the micro-environment. Such interactions have led to the development of the field of optical imaging which encompasses a wide variety of methods and approaches (Table 3), from visualising tissue anatomy on the microscopic scale (Zonios et al., 2001) to the 3D localisation of a photonic signal in whole animals using fluorescence molecular tomography (Ntziachristos, 2006).

In this chapter we will focus on biophotonic imaging (BPI), a preclinical imaging technique based on the ability of light to travel through flesh. This principle is easily demonstrated by placing a torch underneath ones hand and observing the light emerging through the fingers. BPI involves the detection of visible light which arises from either the excitation of a

fluorescent protein (FP), or molecule, or from an enzyme-catalysed oxidation reaction (a phenomenon known as bioluminescence).

Resolution	Technique	Contrast	Depth
Microscopic	Epi microscopy	A, Fl	20 μm
	Confocal microscopy	Fl	500 μm
	Multi-photon microscopy	Fl	800 μm
Mesoscopic	Optical projection tomography	A, Fl	15 mm
	Optical coherence tomography	S	2 mm
	Laser speckle imaging	S	1 mm
Macroscopic	Hyperspectral imaging	A, S, Fl	<5 mm
	Endoscopy	A, S, Fl	<5 mm
	Fluorescence reflectance imaging (FRI)	A, Fl	<7 mm
	Diffuse optical tomography (DOT)	A, Fl	<20 cm
	Fluorescence resonance imaging (FRI)	A, Fl	<7 mm
	Fluorescence molecular tomography (FMT)	Fl	<20 cm
	Biophotonic Imaging (BPI)	Fl, E	< 3cm

Key: A, Absorption; Fl, fluorescence; S, Scattering; E, Emission.

Table 3. Optical imaging techniques (taken from N. Andreu et al., 2011).

Bioluminescence arises from the oxidation of a substrate (a luciferin) by an enzyme (a luciferase), which usually requires energy (in the form of $FMNH_2$ and ATP) and oxygen. Luciferin and luciferase are generic terms as none of the major classes share sequence homology. Most widely studied are the systems belonging to luminous beetles in the family Lampyridae (such as the firefly *Photinus pyralis*), the sea pansy *Renilla reniformans*, the marine copepod *Gaussia princeps* and numerous luminous bacteria (such as *Vibrio* sp. and *Photorhabdus luminescens*). In contrast, fluorescence arises when a fluorescent compound is irradiated with light of a suitable wavelength. This leads to the transition of an electron in the molecule to a higher energy state, a process known as excitation. This process is almost instantaneous, taking around 10^{-15} seconds. Upon return of the electron to a lower energy level (around 10 ns), light of lower energy is emitted, giving the fluorescent signal.

Although the emitted light may be dim, it can be detected externally using sensitive photon detectors such as those based on cooled, or intensified, charge coupled device (CCD) cameras, mounted within light-tight specimen chambers. As light passes through a range of tissue types (including skin, muscle and bone) it is possible to observe and quantify the spatial and temporal distribution of light production from within living subjects (N. Andreu et al, 2011). In general, imaging of luminescence is much more sensitive than imaging fluorescence as a result of better signal-to-noise ratios. This is mainly due to the high levels of background fluorescence *in vivo* compared to luminescence, due to endogenously produced fluorophores such as keratin, porphyrins, NAD(P)H, collagen and elastin (Troy et al., 2004). A major limitation of BPI is the limited depth penetration through tissue. Hence BPI is currently only applied to imaging small animals, although visualisation of bioluminescence from within infant monkeys (the long-tailed macaque, *Macaca fascicularis*) has been reported (Tarantal et al., 2006). Alternatively, the light could potentially be detected internally using an endoscopic device, such as reported by Hsiung and colleagues

to image colonic pathology (Hsiung et al., 2008). The advantages of BPI are that it is inexpensive, sensitive and requires short imaging times.

3. Use of molecular imaging in animal models of TB

M. tuberculosis, the infectious agent of TB, can infect many animals in addition to its natural human host. Although the study of TB in patients is extremely useful, a detailed analysis of the pathogenesis and the interactions of *M. tuberculosis* with the host requires the use of well-defined models that can be infected in a controlled manner. Furthermore, animal models can be easily manipulated, can be used in statistically significant numbers, and the results are obtained in a relatively short time frame. In addition, they are particularly useful in drug and vaccine efficacy testing before moving the most promising candidates to clinical studies.

For both practical and economical reasons, laboratory mice remain the most extensively used animal model of TB: they are easy to manipulate and house, there is a wide range of mutant and genetically modified strains, and there are many immunological reagents available. However, latent infection is difficult to achieve in the mouse model, and the pathology, with poorly organised granulomas, differs considerably to that observed in humans. By contrast, guinea pigs and particularly rabbits display a spectrum of pathology that better represents the human disease. Moreover, guinea pigs are extremely susceptible to *M. tuberculosis* infection and relatively inexpensive compared to other larger animal models, which makes this model very useful for vaccine efficacy studies. Even so, studies with guinea pigs and rabbits are limited by the narrow range of immunological reagents available. This is not the case in non-human primates, which are the closest model to humans in terms of pathology and disease development and therefore constitute the most relevant model to predict treatment and vaccine efficacy. Nevertheless, work with non-human primates presents many limitations regarding space requirements, animal availability, and costs. In summary, each animal model presents both advantages and disadvantages which must be carefully considered when designing a new study. A more detailed description of these animal models of TB can be found elsewhere (Dharmadhikari & Nardell, 2008; Flynn, 2006; Gupta & Katoch, 2005).

The use of animals in research is accompanied by ethical responsibilities and most countries promote the three Rs: replacement, reduction and refinement. Replacement refers to methods that avoid the use of animals, for example, *in silico* computer modelling, or using established human and animal cell lines and non-mammalian models such as the nematode *Caenorhabditis elegans* or the embryo of the zebrafish, *Danio rerio*. Reduction refers to methods which minimise the use of animals and enable researchers to obtain comparable levels of information from fewer animals or to obtain more information from the same number of animals, thereby reducing the future use of animals. Refinement refers to improvements to scientific procedures and husbandry which minimise actual or potential pain, suffering, distress or lasting harm and/or improve animal welfare. Molecular imaging is a very powerful tool for implementation of two of the 3Rs, refinement and reduction. Using traditional disease models, infected animals are sacrificed at defined time points and tissues excised for determination of pathogen numbers and localisation. In contrast, the non-destructive nature of molecular imaging allows the course of an infection to be monitored simply by repeated imaging of the same group of animals. Importantly, this allows disease

progression to be followed with extreme accuracy, while allowing each animal to act as its own control. Furthermore, we have demonstrated that BPI can provide real time information on the effectiveness of the inoculation method (Wiles et al., 2007). As a result, errors in administration can be detected immediately (N. Andreu et al., 2011) and animals eliminated from further study – thus minimising any potential pain, suffering and distress for the animal and reducing variation by removing flawed scientific data.

One major drawback to working with *M. tuberculosis* is the slow growth of the organism. This lengthens the time required to carry out *in vivo* experiments extraordinarily, and delays the quantification of bacterial burdens by about four weeks, which is the time required for *M. tuberculosis* to form visible colonies on agar. Therefore, the use of molecular imaging to track infection dynamics in real time would be a major advantage as it would enable researchers to make on-the-spot decisions, shortening the length of the experiment if clear differences (for example, between control and vaccinated groups) were observed. There is, therefore, an increasing interest in the development of molecular imaging techniques in animal models of TB. Moreover, the developments and knowledge acquired through the use of these techniques in animal models may eventually translate into the clinic.

3.1 Computed Tomography (CT)

CT imaging has mostly been used as a complementary technique to PET and SPECT imaging (see sections 3.3 and 3.4), as it gives high-resolution anatomical information for a better localisation of the radionuclide signal. However, CT has also been evaluated as an imaging method on its own to assess disease burden in macaques (Lewinsohn et al., 2006). To this end, four animals were infected by bronchoscopy instillation of *M. tuberculosis*, and disease progression was monitored every four weeks clinically (weight, body temperature, complete blood count and erythrocyte sedimentation rate), immunologically (ELISPOT), bacteriologically (quantitative *M. tuberculosis* culture from bronchoalveolar lavage), and by CT imaging. In addition, a necropsy was performed at the end of the experiment (12 weeks post-infection) which included histopathology and bacterial burden quantification from selected organs. Clinical indicators failed to provide information about disease progression, as most of them were fairly constant through the whole experiment. Most bacterial cultures from bronchoalveolar lavage were positive, although some cultures were negative even though CT imaging and post-mortem analysis showed infection. Even bacterial cultures from post-mortem lung samples were not consistently positive, which was attributed to a non-uniform infection of the lungs and therefore biased tissue sampling. In contrast, CT imaging provided a reliable readout of disease progression in the whole lung and also allowed monitoring of other organs, such as the liver and spleen. Moreover, different types of lesions were observed, and progression of the lesions from small nodules to cavitation and necrosis was evident. CT findings were corroborated by post-mortem histopathology and, together with immunological monitoring, provided a non-invasive, accurate, and rapid assessment of TB in this animal model. It is important to note that even though a CT scanner was not available in the animal biosafety level 3 (BSL3) containment facility, the authors were able to image infected animals in a scanner localised within a non-containment facility, by transporting and imaging the anesthetised macaques in a box fitted with HEPA filters. This is a solution that has also been adopted for other imaging techniques like PET/CT, SPECT/CT and BPI (see below).

3.2 Magnetic Resonance Imaging (MRI)

To our knowledge, MRI was the first molecular imaging method reported for an animal model of TB, when Kraft and colleagues used the technique to assess lesion distribution and lesion numbers as an indication of disease burden in BCG-vaccinated and unvaccinated guinea pigs infected with *M. tuberculosis* by the aerosol route (Kraft et al., 2004). 3D lung images were reconstructed from images taken of 2 mm slices of formalin-fixed and agarose-embedded lungs, and lung volumes, lymph node volumes and total nodular burden were quantified. Small nodules were observed 15 days post-infection, which developed into granulomatous lesions 20 days later. Lesions were uniformly distributed in the lungs, which suggested that aerosol delivery of *M. tuberculosis* results in a homogenous infection. Additionally, lesions numbers supported the hypothesis that a single bacillus establishes a single lesion. In terms of vaccine efficacy, the authors found the same number of lesions in vaccinated and unvaccinated animals but the lesions were smaller in the vaccinated group, thus suggesting that BCG has an effect on disease development rather than on the initial establishment of the infection. All in all, they found that MRI was a useful method to assess disease burden in terms of lesion distribution, size and number. The main limitation was a low sensitivity when dealing with very small (< 1 mm) lesions.

More recently, the same laboratory used MRI to assess treatment efficacy in guinea pigs infected with *M. tuberculosis* (Ordway et al., 2010). The treatment had a dramatic effect on bacterial load with a 4-6 log decrease in viable counts (as determined by colony forming units [CFUs]) both in the lungs and lymph nodes in just 25 days. However, the effect on lesion burden, as quantified by MRI, was slower and could only be detected in the lungs after 50 days of therapy (Figure 1). In addition, the lesions in the lymph nodes of the treated group were smaller, although the differences with the untreated group were only obvious at later time points. These results were corroborated by histological analysis, although the number of lesions in the lungs of the treated animals was already lower than in the control group by day 25.

MRI has also been applied to studies in non-human primates (Sharpe et al., 2009, 2010). Disease burden in this animal model has been traditionally assessed by a range of ante- and post-mortem methods such as clinical signs (behaviour, weight, and body temperature), laboratory markers (haemoglobin levels, erythrocyte sedimentation rate, and immunology),

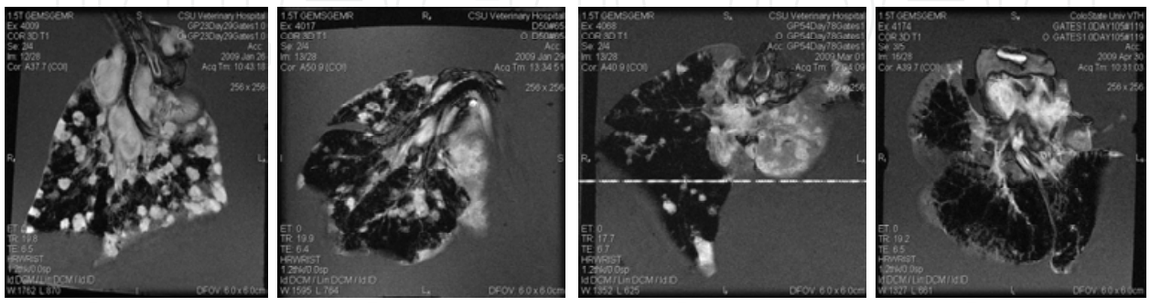

Fig. 1. MRI showing lesions resolving/disappearing during treatment of *M. tuberculosis*-infected guinea pigs with a cocktail of anti-TB drugs (given as days post-treatment).

chest x-ray, gross pathology, and histology. However, most of these methods are qualitative and subjective. Moreover, the most common alternative method, the quantitative estimation of total lesion numbers in the lung by manual counting, is laborious and particularly difficult in animals with more severe disease, as individual lesions become difficult to distinguish. Sharpe and colleagues used MRI and stereology (a statistical method that extracts quantitative information of a 3D structure from measurements made on planar sections of the material) to quantify lesion volume relative to lung volume in macaques infected with a range of doses of *M. tuberculosis* by the aerosol route (Sharpe et al., 2009). Similarly to what was previously seen in guinea pigs, the authors observed a uniform distribution of lesions in the lungs. In addition, the lesion-to-lung volume ratio increased with the infectious dose, and this ratio revealed subtle differences in the level of pulmonary disease and correlated well with other measures of disease burden. By contrast, methods such as gross pathology and chest x-ray were less sensitive and did not differentiate between the levels of disease in the animals exposed to the highest infectious doses. In conclusion, MRI together with stereology makes up a sensitive, quantitative, systematic and consistent method to assess disease burden in the macaque model of tuberculosis. Moreover, when MRI was compared with more traditional methods to measure vaccine efficacy, it was found that MRI combined with stereology was the only readout that distinguished between the unvaccinated and the vaccinated groups, and it was even able to show differences between survivor and non-survivor animals within the vaccinated groups, thus highlighting the sensitivity of the method (Sharpe et al., 2010).

In summary, the use of MRI appears to be a reliable method to assess disease burden in the lungs of *M. tuberculosis*-infected animals. However, it should be noted that the studies described here were performed on fixed lungs where the bacteria had been inactivated, as the use of MRI under BSL3 containment was not available. Initially, the whole lung was fixed and used for imaging to reduce sample error. As a result the tissue could not be used for other procedures, such as determination of bacterial load. However, the results discussed above illustrate that aerosol delivery of *M. tuberculosis* results in an even distribution of the lesions in the lungs and, therefore, samples can be taken and used for other techniques without compromising its reliability. Similarly to what has been done to image live animals by CT scanning, MRI of live animals could be done by using a sealed box with filters to transport the animals to the MRI facility and contain them during imaging. When available, MRI of live animals will allow longitudinal monitoring of disease progression, and real-time observation of vaccine and drug efficacy. The *ex vivo* results discussed here, together with the excellent soft tissue contrast of MRI and the development of faster MRI devices that reduce the artefacts induced by respiratory motion, suggest that *in vivo* MRI may become a very useful technique for the study of TB in animal models.

3.3 Positron Emission Tomography (PET)

Another technique which is gaining popularity in TB research is PET combined with CT imaging (PET/CT). The PET radiotracer [^{18}F]-FDG is used to image inflammation at the infection site, as it accumulates in inflammatory cells such as neutrophils and activated macrophages. This technology has been used to image TB infection (Figure 2) and to assess drug treatment efficacy in mice (Davis et al., 2009b). The authors infected two strains of mice, BALB/c (which develop diffused granulomas) and C3HeB/FeJ (which develop well-

defined necrotic granulomas), and evaluated three different treatments: (i) first line tuberculosis regimen (rifampin + pyrazinamide + isoniazid), (ii) a more bactericidal regimen (rifampin + pyrazinamide + moxifloxacin), and (iii) a bacteriostatic regimen (ethambutol). The animals were imaged and CFUs obtained at different time points during the 12 weeks of treatment. Furthermore, one group of BALB/c mice was followed for 22 weeks after completion of the bactericidal treatments to assess relapse of the infection. For the imaging, anesthetised mice were contained in a sealed device with holes for passage of gases fitted with 0.22 μm filters. In both mouse models, CFU counts perfectly reflected the efficiency of the three treatments being evaluated, with a faster decrease in bacterial numbers when moxifloxacin was used instead of isoniazid, and stabilization of bacterial burden when mice were treated with ethambutol only.

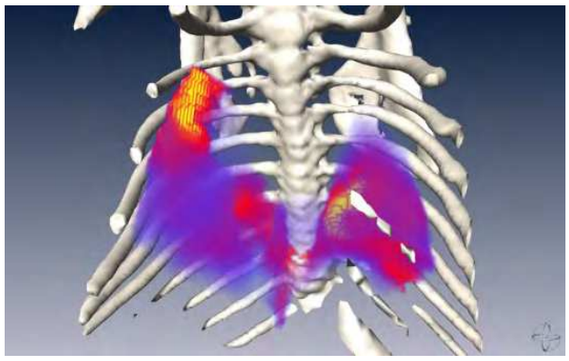

Fig. 2. 3D co-registered PET and CT images from a live C3HeB/FeJ mouse infected with a low-dose aerosol of *M. tuberculosis*. The brightness of the lesions represents FDG activity, with brighter lesions being more active. The heart also takes up FDG and can therefore be seen on the left. The bony structure (rib cage and scapula), shown in grey, were extracted from the CT (Davis, S.L. & Jain, S.K.; unpublished data).

The use of PET/CT imaging allowed differentiation between the bacteriostatic and bactericidal treatments, as the [^{18}F]-FDG activity was higher in the mice treated with ethambutol. However, unexpectedly, [^{18}F]-FDG activity was higher in mice treated with moxifloxacin than in those treated with isoniazid during the first four weeks of treatment. The authors suggested that this could be due to the limited statistical power of the study since only three mice per group were used, or that it could be an inherent limitation of using [^{18}F]-FDG, whereby an increased killing of *M. tuberculosis* would cause an increased Tumour Necrosis Factor (TNF)-mediated inflammation and therefore increased [^{18}F]-FDG activity even though bacterial numbers were decreasing. Relapse was detected in both groups of mice by PET imaging and by CFU counts. In summary, PET/CT allowed the non-invasive monitoring of disease progression in real-time. Moreover, individual lesions could be observed in the C3HeB/FeJ mouse model; as treatment response has been suggested to be lesion-dependent, the possibility of monitoring individual lesions would be very useful. However, it is important to take into account that this method does not specifically image infection but only measures inflammation which, as illustrated by the treatment results of this work, does not always correlate with bacterial burden. Nevertheless, this method has some advantages over using, for example, CFU counts: it uses a reduced number of animals, and the same animals can be repeatedly imaged which allows a more easy detection of untimed events such as relapse.

PET/CT imaging is also being used in non-human primates, although the results have only been presented in meetings and no peer-reviewed article has been published to date. For example, PET/CT has been used to monitor disease progression and drug efficacy in macaques (Lin et al., 2009). Using CT imaging, lesions as small as 1 mm were detected in the lungs and lymph nodes of infected animals. Moreover, lesion progression could be followed over time. Interestingly, co-registered [^{18}F]-FDG–PET images revealed that individual granulomas differed in their [^{18}F]-FDG affinity: whereas some granulomas exhibited high uptake values, others seemed devoid of [^{18}F]-FDG. The imaging results were complemented with post-mortem histology and bacterial burden analysis of individual lesions. The authors found a complex, lesion-specific response to drug treatment that included changes in [^{18}F]-FDG avidity. These remarkable results show that even though PET and CT are two complementary techniques, images should be first analysed separately, and that caution should be taken when interpreting the results of PET activity in terms of [^{18}F]-FDG accumulation.

3.4 Single Photon Emission Computed Tomography (SPECT)

SPECT/CT has also been used for imaging of TB infection in mice (Davis et al., 2009a). The authors used the radiotracer 1-(2′deoxy-2′-fluoro-β-D-arabinofuranosyl)-5-[^{125}I]-iodouracil ([^{125}I]-FIAU), a nucleoside analogue, together with an engineered *M. tuberculosis* strain that stably expressed the enzyme thymidine kinase (TK) which phosphorylates [^{125}I]-FIAU leading to its accumulation within the bacteria. In contrast to [^{18}F]-FDG–PET imaging, this technique specifically images the bacteria instead of the inflammatory response, as [^{125}I]-FIAU is a poor substrate for mammalian TK. Using this technique, the authors were able to image individual necrotic granulomas in the lungs of C3HeB/FeJ infected mice (Figure 3). The presence of the lesions was subsequently corroborated by histopathology. However, the limit of detection was found to be $5x10^6$ to $1x10^7$ CFUs, a rather high bacterial burden for mice infected with *M. tuberculosis*. The authors suggested that the sensitivity of the method could be improved by increasing the expression of TK in the bacilli or by using more

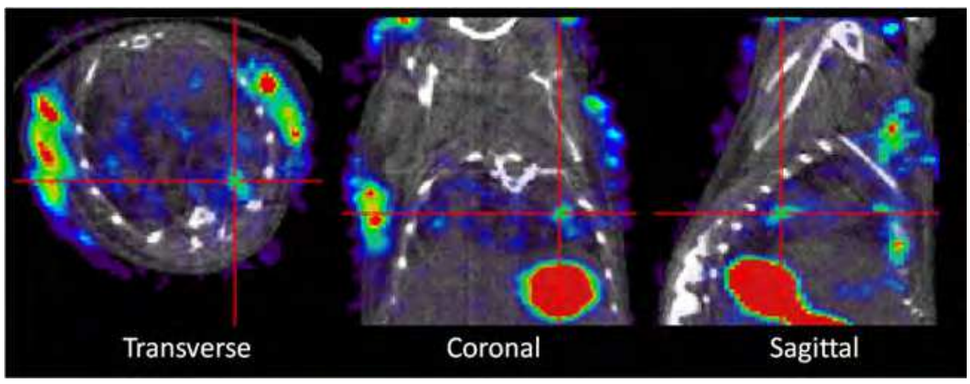

Fig. 3. Co-registered SPECT and CT images from a live C3HeB/FeJ mouse infected with a low-dose aerosol of an *M. tuberculosis* strain expressing bacterial thymidine kinase (TK) under the control of a strong mycobacterial promoter. TB lesions were imaged 8-weeks after this infection, using [^{125}I]-FIAU, a nucleoside analog substrate for bacterial TK. The FIAU-SPECT signal localizes to the TB lesion (crosshairs) in the lungs, indicating uptake of FIAU by the bacteria (Davis, S.L. & Jain, S.K.; unpublished data).

sensitive (and expensive) radionuclides such as ^{123}I or ^{124}I. Other limitations of the technique include: the limited blood supply at the centre of the granulomas could limit accessibility to imaging substrates; TK requires ATP, which could be restricted in latent bacteria; and the presence of non-specific signal in tissues such as liver, gall bladder, or stomach, that either metabolize or excrete FIAU or its iodinated derivatives.

3.5 Biophotonic Imaging (BPI)

Bioluminescence imaging is one of the most widely used imaging techniques in the study of infectious diseases (N. Andreu et al., 2011). Luciferases have been used in mycobacterial research for more than 20 years; the two most widely used are the firefly luciferase (FFluc) and the luciferase of the bacterium *Vibrio harveyi* (LuxAB). Both luciferases produce light in the presence of a combination of a substrate and a cofactor, namely D-luciferin and ATP (for FFluc) and n-decanal and $FMNH_2$ (for LuxAB). As the co-factors are only found in live cells, the production of light by the luciferases provides a sensitive indicator of cell viability. The bacterial luciferase system has a major advantage when compared with the FFluc: the genes for the synthesis of the substrate are known and can be co-expressed with the *luxAB* genes as a convenient gene set (*luxCABDE*) that renders the bacteria autoluminescent, that is, no external addition of substrate is needed for light production. Light-emitting mycobacteria have been used as an easier and faster approach than commonly used methods to assess bacterial numbers *in vitro* and in macrophages, for example, in drug screening assays (Arain et al., 1996). The first approach to use luminescent mycobacteria in animal models consisted of measuring luminescence *ex vivo* in organ homogenates (Hickey et al., 1996). This method generated results in a much quicker time frame than using CFU counts and has been applied to drug and vaccine efficacy testing (Hickey et al., 1996; Snewin et al., 1999).

More recently, a recombinant *M. bovis* BCG strain expressing the bacterial luciferase enzyme LuxAB has been used to monitor mycobacterial infection *in vivo* (Heuts et al., 2009). In this work, only the luciferase genes were expressed and, therefore, the n-decanal substrate had to be injected before imaging. Although n-decanal is very toxic, the authors were able to deliver it dissolved in a mixture of olive oil and ethanol by injection into the mouse peritoneum. To assess the usefulness of the system, immunodeficient $RAG2^{-/-}/\gamma cR^{-/-}$ mice were intravenously infected with the luminescent BCG strain, and bioluminescence imaging was performed at different time points for 11 weeks. A signal coming from the spleen was detected four weeks post-infection, when the bacterial load was around $5x10^7$ CFUs. The signal increased over time and extended to the abdomen of the animal but no signal was observed in the lungs, even though CFU counting showed a bacterial burden in this organ of 10^7 CFUs at eight weeks post-infection. However, luminescence was detected in the excised lungs, suggesting that tissue attenuation was responsible for the failure to detect the signal in the whole animal. The same luminescent BCG strain was also used to assess drug efficacy and the host immune response. A reduction in light emission, which paralleled the reduction in bacterial numbers, was observed in treated mice compared to the untreated mice, as well as in inmunocompetent BALB/c and T-cell reconstituted $RAG2^{-/-}/\gamma cR^{-/-}$ mice compared to immunosupressed $RAG2^{-/-}/\gamma cR^{-/-}$ mice. Therefore, bioluminescence imaging allows monitoring of mycobacterial infection in mice. However, the system was not useful for imaging infection in the lungs, and a toxic substrate had to be administered to the mice before imaging.

To overcome these difficulties, our group has recently optimised the expression of FFluc and the complete bacterial luciferase system in *M. tuberculosis* (N. Andreu et al., 2010). The resulting mycobacterial strains express either the optimised gene encoding FFluc (which is the brightest luciferase and uses a non-toxic substrate) or the optimised *luxCABDE* gene set from *Photorhabdus luminescens* (which results in autoluminescent strains that do not need the exogenous addition of substrate to produce light). Both *M. tuberculosis* strains were imaged *in vivo* in the lungs and spleens of infected mice (Figure 4), with limits of detection of around 10^5-10^6 CFU per lung and 10^5 CFU per spleen, whereas as few as 10^4 CFU can be imaged in the dissected organs (our unpublished results). Further work will assess the usefulness of these luminescent mycobacteria in drug efficacy testing and in other small animal models such as guinea pigs.

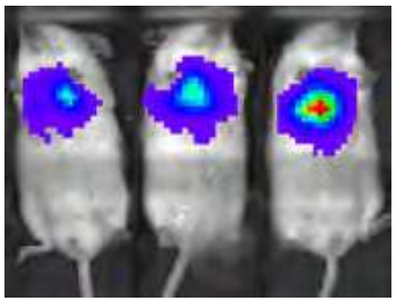

Fig. 4. Visualisation of bioluminescent bacteria within living mice infected with *FFluc*-expressing *M. tuberculosis* after administration of luciferin. The image was obtained using an IVIS Spectrum and is displayed as a pseudocolour image, where red represents the most intense light emission while blue correspond to the weakest signal (Andreu, N. & Wiles, S; unpublished data).

Fluorescence imaging has had a more limited use in the study of infectious diseases, although it has been widely applied to other research fields such as cancer research (N. Andreu et al., 2011). In a first attempt to develop fluorescence imaging of *M. tuberculosis* infection, a GFP-expressing *M. tuberculosis* strain was used to infect mice and guinea pigs, and five weeks post-infection the lungs were imaged using a photon imager (Sugawara et al., 2006). Granulomas as small as 1 mm of diameter were detected, and the results were corroborated by histopathology examination. The same fluorescence technique was used to visualize granulomas in a latent model of TB in guinea pigs (Sugawara et al., 2009). In this case, the animals were subcutaneously infected with *M. tuberculosis* and the infection was followed for 10 months. No clinical signs of infection were evident in any of the animals for the length of the experiment, although the bacteriological analysis of lungs and spleens 180 and 300 days post-infection showed the presence of a few bacteria. Similarly, even though no granulomas were detected by gross pathology examination, microgranulomas were observed in the histological analysis. According to the authors, these small lesions corresponded to the fluorescent spots detected by photon imaging of sliced lungs and spleens. More work is still needed to validate these results and to be able to use this technology *in vivo*.

FPs that emit light in the far-red region of the spectrum are more appropriate for *in vivo* imaging than for example GFP, as red light is less affected by absorption and scattering

when travelling through tissues. This is exemplified by the finding that as few as 10^5 CFUs of a BCG strain that expressed tdTomato (excitation 554 nm, emission 581 nm) can be detected after being subcutaneously injected into mice, in comparison to 10^7 CFUs of BCG expressing enhanced GFP (EGFP) (excitation 484 nm, emission 510 nm) (Kong et al., 2009). Therefore, far-red reporters show a lot of promise for fluorescence *in vivo* imaging of *M. tuberculosis* infection in animal models, and the expression of several red FPs in mycobacteria has recently been optimised (Carroll et al., 2010).

The strategies presented above use recombinant bacteria that express an exogenous FP. A much more versatile strategy consists of using an activatable fluorescent agent that is non-fluorescent in its native (quenched) state but produces fluorescence through enzyme-mediated release of its fluorochrome. This strategy has been widely used in cancer and inflammation research but, until recently, not in infectious diseases. Using a near-infrared fluorogenic substrate for β-lactamase, an enzyme that is endogenously expressed by *M. tuberculosis* but not by eukaryotic cells, it is possible to detect 10^6 CFUs of *M. tuberculosis* subcutaneously injected in mice (Kong et al., 2010). The maximal signal was produced 48 h after substrate injection, and no signal was detected 48 h later, which suggests that repetitive imaging of the same animals can be done every 96 h. Surprisingly, the limit of the detection in the lungs of live animals was 10^4 CFUs, which is far lower than the limit of detection subcutaneously, even though the lungs are localised much deeper in the body. The signal was localised laterally, close to the armpit of the animal, and 3D fluorescence molecular tomography (FMT) and imaging of the excised lungs proved that the lungs were the source of the signal. The amount of fluorescence correlated with bacterial numbers when the imaging was performed 24 h post-substrate administration, but at later time-points substrate accumulation lead to a similar level of fluorescence independently of bacterial numbers. In addition, the technique was used to assess drug efficacy by imaging treated and untreated mice, showing that the signal increased in the untreated group while it decreased in the treated group. Although much work needs to be done to assess the usefulness of the technique, one can imagine many potential applications not only in *in vivo* imaging but also *in vitro* using fluorescence microscropy or FACS, as well as for TB diagnosis (e.g. detection of bacilli in sputum or imaging tuberculosis in patients). However, a limitation that needs to be considered is the fact that other bacteria, such as *Pseudomonas aeruginosa* or *Staphylococcus aureus*, also express β-lactamase and therefore may give a false signal. Thus, alternative fluorogenic substrates that are activated by other endogenous enzymes are currently under study; for example, certain trehalose analogues that are substrates for the *M. tuberculosis* mycolyltransesterases Ag85A, Ag85B and Ag85C (Backus et al., 2011).

4. Imaging TB in human disease

4.1 Radiography

The plain radiograph was first described in 1895 by Röntgen, at the same time that the TB pandemic was peaking in wealthy Western countries such as Victorian England. Consequently, there is a long experience and literature of plain radiographic imaging of TB, which has been reviewed previously (McAdams et al., 1995; J. Andreu et al., 2004; Curvo-Semedo et al., 2005). In summary, TB can cause a wide array of chest x-ray appearances, but classically causes consolidation and cavitation in the apices of the upper lobes. TB can also cause disease at the apices of the lower lobes, which appears in the mid-zone on chest

radiograph (Figure 5). However, TB can result in a wide range of other features, such as miliary disease with small millet seed-sized nodules throughout the lungs, pleural effusions, mediastinal lymphadenopathy and extrapulmonary disease. In the era of HIV infection, where the host immune system is compromised, the appearances of pulmonary TB are often atypical (Kwan & Ernst, 2011), ranging from classical cavitation to areas of pneumonia to a normal chest x-ray even in the presence of a high mycobacterial load. This illustrates the importance of the adaptive immune response in driving lung inflammation, resulting in consolidation and tissue destruction.

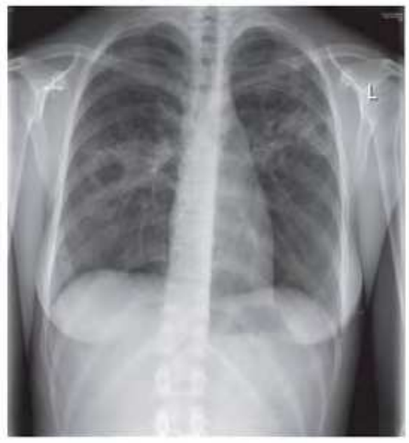

Fig. 5. Radiograph illustrating right mid zone cavitation on a 17 year old patient with pulmonary TB.

As TB is treated, areas of consolidation tend to gradually resolve, leaving an area of fibrosis or scar tissue which persists for life. Cavities remain even after cure, because the lung cannot reconstruct the intricate extracellular matrix after it has been destroyed. However, it is well recognised that radiographic appearances may often worsen before they improve (Leung, 1999), and similarly some lesions may increase in size and density while others appear to resolve. Even in HIV negative patients with drug-sensitive disease, such "paradoxical" reactions may occur (Cheng, 2002). This demonstrates the different behaviour of inflammatory lesions even in the same patient, and one challenge for modern imaging techniques is to define the molecular mechanisms underlying this immune response to improve our understanding of what constitutes an effective as opposed to deleterious immune response to TB.

4.2 Computed Tomography (CT)

CT involves cross-sectional imaging of patients and so permits a much greater degree of resolution of anatomical structures, although it results in a higher radiation dose and higher cost than plain radiography. CT can demonstrate cavity formation with much greater sensitivity and will demonstrate subtle changes which may be missed on plain chest x-rays (Figure 6 [left panel]). For example, filling of small airways with inflammatory debris may result in a "tree-in-bud" pattern (Figure 6 [right panel], arrow), which should immediately alert the physician to the possibility of mycobacterial infection. Therefore, CT scanning provides information of changes at a much more precise anatomical level than plain

radiography, but does not give information about the molecular events occurring at the site of infection.

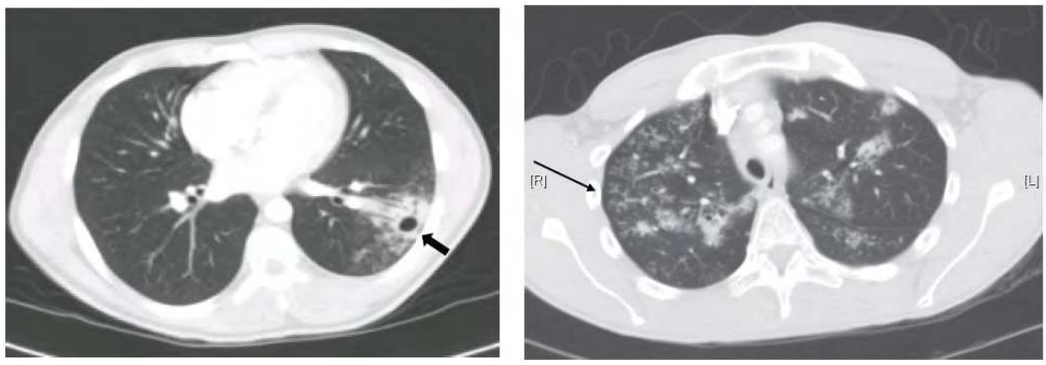

Fig. 6. CT imaging reveals a small left mid zone cavity (indicated by arrow) that was not visible on plain chest x-ray (left panel) and a tree-in-bud bronchial filling in a 33 year old man with pulmonary TB (right panel), which appears as branched opacities in the lung field adjacent to arrowhead.

4.3 Magnetic Resonance Imaging (MRI)

MRI provides the best imaging of the meninges and spinal cord, and so is useful in the diagnosis of cerebral TB, TB meningitis and paraspinal TB abscesses. MRI is a rapidly developing area, and so may emerge as a modality which can provide insight into molecular events in TB. The advantage of MRI is that it involves no ionizing radiation and provides excellent anatomical resolution. New MRI modalities to investigate inflammatory diseases are under development (Pirko et al., 2004), but these have not yet entered the clinical arena for investigation in TB.

4.4 Positron Emission Tomography (PET)

PET imaging is a widely used nuclear medicine technique which has the potential to study pathological events at a molecular level before extensive anatomical changes are observed on plain radiography. PET imaging is commonly combined with CT scanning in patients to provide both functional and anatomical information. [^{18}F]-FDG accumulates in metabolically active cells after phosphorylation, and so is taken up by metabolically active macrophages within the TB granuloma and other inflammatory foci. A primary limitation of PET imaging for TB is the high cost and low availability in developing world. Increased PET uptake is well described in both pulmonary and extrapulmonary TB lesions (Matsuura et al., 2000; Bakheet et al., 1998; C.M. Yang et al., 2003), and can cause diagnostic uncertainty with malignancy and other infections (Chen et al., 2004; Li et al., 2008).

PET scanning is clinically useful in certain patients with TB. For example, when patients have normal radiology but symptoms highly suggestive of active TB, PET scans may identify occult foci of infection which can then be sampled to confirm the diagnosis and for culture (Figure 7, arrow). Furthermore, PET imaging has been proposed for monitoring the resolution of TB disease (Hofmeyr et al., 2007), although the benefit must be weighed against the increased radiation exposure. Current research questions which need to be

addressed are whether PET imaging can be useful to define cure, especially in the context of drug-resistant TB where treatment regimes may exceed 18 months, and also investigate whether active foci can be identified in patients with clinically "latent" disease.

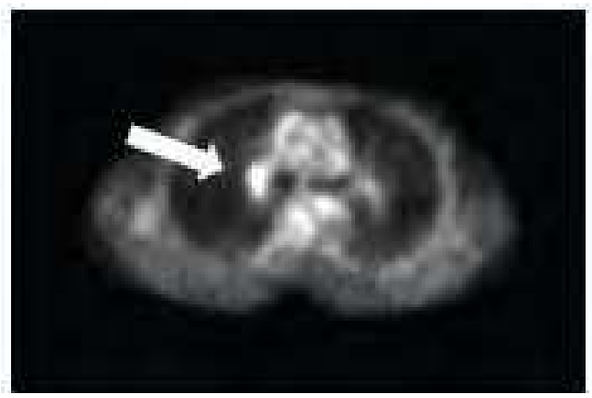

Fig. 7. PET imaging reveals increased uptake of [^{18}F]-FDG in a right hilar lymph node, appearing as bright white (as indicated by arrow).

In addition to [^{18}F]-FDG, a wide array of radiopharmaceuticals have been developed at the preclinical level which might be applied to TB (Signore & Glaudemans, 2011). However, the potential of these in man have not yet been confirmed. For example, radiolabelling the antibiotic ciprofloxacin looked promising initially to investigate cryptic foci of infection (Britton et al., 2002), but has not entered clinical practice widely. The ability to detect a wide range of pathophysiological markers suggests that PET imaging may emerge as a powerful modality to investigate the biology of TB in man, but currently most prospective candidates require further study in model systems before clinical studies in man can be considered.

4.5 Single Photon Emission Computed Tomography (SPECT)

A number of SPECT radiotracers have been applied to the management of TB including ^{99m}Tc-methoxyisobutylisonitrile (^{99m}Tc-MIBI) (Ahmadihosseini, 2008), ^{67}Ga (Liu et al., 2007) and ^{111}In-octreotide (Vanhagen et al., 1994). ^{99m}Tc-MIBI is a widely used myocardial perfusion agent, which can accumulate in tumours and inflammatory lesions (Aktolun et al., 1991; Caner et al., 1992; Kao et al., 1994; A. Yang et al, 2007). Ahmadihosseini and colleagues studied 36 patients with either proven active or inactive treated pulmonary TB and found that ^{99m}Tc-MIBI uptake was increased in 23 out of 24 patients (95.8%) with active pulmonary TB but none of those with inactive TB (Ahmadihosseini et al., 2008). *M. tuberculosis* has been demonstrated to have significantly higher ^{99m}Tc-MIBI uptake compared with fibroblasts and myocytes cultures (Stefanescu et al., 2007), suggesting the bacilli themselves contribute to the signal detected on ^{99m}Tc-MIBI SPECT images.

A number of studies have found positive SPECT images in sputum smear negative patients subsequently found to have a positive sputum culture for *M. tuberculosis* (Ahmadihosseini et al., 2008; Önsel et al., 1996; Stefanescu et al., 2006), suggesting that SPECT imaging may be very useful while awaiting culture results. However, as previously stated, many benign and malignant etiologies can also demonstrate ^{99m}Tc-MIBI uptake (Aktolun et al., 1991; Caner et

al., 1992; Kao et al., 1994; A. Yang et al, 2007), which significantly decreases the value of this radiotracer in the differential diagnosis of pulmonary TB from other lung pathologies.

5. Future prospects

A fundamental challenge of TB research is to develop applications which are useful in resource poor settings and can be deployed with minimal investment in infrastructure, maintenance and staff expertise. Furthermore, any application needs to be equally applicable in urban and rural settings. Most modern imaging techniques are useful in the developed world, but are not available to the vast majority of patients with TB who live in resource-poor settings.

However, the detailed study of a small number of patients may identify pathophysiological markers of TB which can then be simplified to develop new diagnostic and therapeutic approaches applicable in resource poor settings. Ironically, when one considers molecular imaging of TB in this light, developing an imaging technique based on plain chest radiography is currently the only widely deliverable approach in the near future. For example, if a highly radio-dense specific TB ligand was developed, a diagnostic test might involve taking an initial chest x-ray, injecting the labelled ligand, and then taking a second x-ray to identify high uptake in the region of TB. This might be useful in the common clinical scenario when a patient presents with upper zone fibrosis, which may be caused by either old self-healed TB or new active TB. If the patient is sputum smear negative, an expensive and invasive bronchoalveolar lavage is required, so a non-invasive test to determine disease activity would be useful.

Another frequent clinical scenario is a patient with immunological evidence of infection, but with a normal chest x-ray and a cryptic location of disease. An investigation whereby one could locate the site of disease for aspiration and culture analysis would be clinically useful. This assay might either rely on antimycobacterial ligands, potentially using the "dock and lock" strategy (Goldenberg et al., 2007), whereby a primary antibody is first injected which docks on the mycobacterial target, and then 24 hours later a second radiolabelled antibody is injected which locks onto the primary antibody, or alternatively might focus on the host immune response, such as looking for increased metalloproteinase activity at the site of disease (Elkington et al., 2011).

In additional to diagnosis, a secondary role of imaging is to determine the prognostic and therapeutic correlates of host immunity. Currently, standard treatment lasts for six months. A recent trial comparing short-course therapy for four months in patients with low risk features was stopped because of increased recurrence in the short course treatment group (Daley, 2010). We need better markers to identify patients who will respond rapidly to treatment and imaging modalities to define mycobacterial load, the effectiveness of the host immune response and TB cure.

6. Conclusions

It is clear that molecular imaging technologies will play an important role in improving our understanding of the host-pathogen interactions that occur in animal models of TB, and should speed up preclinical testing of novel vaccine candidates and therapeutic regimes. In

the clinical setting, standard radiographic imaging is likely to remain the mainstay of TB management in humans, with PET imaging emerging as a useful adjunct in specific cases. Indeed, molecular imaging in human TB also has the potential to provide valuable insights into disease pathogenesis, and to aid in the development of new diagnostic approaches and treatment options. However, it remains to be discovered whether approaches currently at preclinical development can be rolled out to the regions of the world where TB is pandemic. We hope that the detailed investigation of small number of patients using cutting-edge technologies may identify pathological markers which can then be developed into simpler, plain radiograph based assays which fulfil the requirements of a truly valuable TB diagnostic.

7. Acknowledgements

This work has been supported in part by a grant to the Imaging TB consortium from the Bill and Melinda Gates Foundation TB Drug Accelerator Program. PE is funded by the UK National Institute for Health Research (NIHR) and is grateful for support from the NIHR Biomedical Research Centre (BRC) scheme at Imperial College London. SW is funded by a Sir Charles Hercus Fellowship from the Health Research Council of New Zealand. The authors would like to thank Prof. Ian Orme (Colorado State University) and Dr. Sanjay Jain MD (Johns Hopkins) for the provision of figures.

8. References

Ahmadihosseini, H., Sadeghi, R., Zakavi, R., Kakhki, V.R. & Kakhki, A.H. (2008). Application of technetium-99m-sestamibi in differentiation of active from inactive pulmonary tuberculosis using a single photon emission computed tomography method. *Nuclear Medicine Communications*, Vol. 29, No. 8, August 2008, pp. 690-694, ISSN 0143-3636

Aktolun, C., Demirel, D., Kir, M., Bayhan, H. & Maden, H.A. (1991). Technetium-99m-MIBI and thallium-201 uptake in pulmonary actinomycosis. *Journal of Nuclear Medicine*, Vol. 32, No. 7, July 1991, pp. 1429–1431, ISSN 0161-5505

Alric, C., Taleb, J., Le Duc, G., Mandon, C., Billotey, C., Le Meur-Herland, A., Brochard, T., Vocanson, F., Janier, M., Perriat, P., Roux, S. & Tillement, O. (2008). Gadolinium chelate coated gold nanoparticles as contrast agents for both X-ray computed tomography and magnetic resonance imaging. *Journal of the American Chemical Society*, Vol. 130, No. 18, May 2008, pp. 5908-5915, ISSN 0002-7863

Andreu, J., Caceres, J., Pallisa, E., and Martinez-Rodriguez, M. (2004). Radiological manifestations of pulmonary tuberculosis. *European Journal of Radiology*, Vol. 51, No. 2, August 2004, pp. 139-149, doi:10.1016/j.ejrad.2004.03.009, ISSN 0720-048X

Andreu, N., Zelmer, A., Fletcher, T., Elkington, P.T., Ward, T.H., Ripoll, J., Parish, T., Bancroft, G.J., Schaible, U., Robertson, B.D. & Wiles, S. (2010). Optimisation of bioluminescent reporters for use with mycobacteria. *PLoS One,* Vol. 5, No. 5, May 2010, e10777, ISSN 1932-6203

Andreu, N., Zelmer, A. & Wiles, S. (2011). Non-invasive biophotonic imaging for studies of infectious disease. *FEMS Microbiology Reviews*, Vol. 35, No. 2, March 2011, pp. 360-394, ISSN 0168-6445

Arain, T. M., Resconi, A.E., Singh, D.C. & Stover, C.K. (1996). Reporter gene technology to assess activity of antimycobacterial agents in macrophages. *Antimicrobial Agents and Chemotherapy,* Vol. 40, No. 6, June 1996, pp. 1542-1544, ISSN 1098-6596

Backus, K.M., Boshoff, H.I., Barry, C.S., Boutureira, O., Patel, M.K., D'Hooge, F., Lee, S.S., Via, L.E., Tahlan, K., Barry, C.E. III & Davis, B.G. (2011). Uptake of unnatural trehalose analogs as a reporter for *Mycobacterium tuberculosis*. *Nature Chemical Biology,* Vol. 7, No. 4, April 2011, pp. 228-235, ISSN 1552-4450

Bakheet, S.M., Powe, J., Ezzat, A., & Rostom, A. (1998). F-18-FDG uptake in tuberculosis. *Clinical Nuclear Medicine*, Vol. 23, No. 11, November 1998, pp. 739-742, ISSN 0143-3636

Britton, K.E., Wareham, D.W., Das, S.S., Solanki, K.K., Amaral, H., Bhatnagar, A., Katamihardja, A.H., Malamitsi, J., Moustafa, H.M., Soroa, V.E., Sundram, F.X. & Padhy, A.K. (2002). Imaging bacterial infection with (99m)Tc-ciprofloxacin (Infecton). *Journal of Clinical Pathology*, Vol. 55, No. 11, November 2001, pp. 817-823, ISSN 0021-9746

Caner, B., Kitapcl, M., Unlu, M., Erbengi, G., Calikoğlu, T., Göğüş, T. & Bekdik, C. (1992). Technetium-99m-MIBI uptake in benign and malignant bone lesions' a comparative study with technetium-99m-MDP. *Journal of Nuclear Medicine*, Vol. 33, No. 3, March 1992; pp. 319–324, ISSN 0161-5505

Carroll, P., Schreuder, L.J., Muwanguzi-Karugaba, J., Wiles, S., Robertson, B.D., Ripoll, J., Ward, T.H., Bancroft, G.J., Schaible, U.E. & Parish, T. (2010). Sensitive detection of gene expression in mycobacteria under replicating and non-replicating conditions using optimized far-red reporters. *PLoS One,* Vol. 5, No. 3, March 2010, e9823, ISSN 1932-6203

Chen, Y.K., Shen, Y.Y. & Kao, C.H. (2004). Abnormal FDG PET imaging in tuberculosis appearing like lymphoma. *Clinical Nuclear Medicine*, Vol. 29, No. 2, February 2004, pp. 124, ISSN 0363-9762

Cheng, V.C., Ho, P.L., Lee, R.A., Chan, K.S., Chan, K.K., Woo, P.C., Lau, S.K., & Yuen, K.Y. (2002). Clinical spectrum of paradoxical deterioration during antituberculosis therapy in non-HIV-infected patients. *European Journal of Clinical Microbiology & Infectious Diseases*, Vol. 21, No. 11, November 2002, pp. 803-809, ISSN 0934-9723

Curvo-Semedo, L., Teixeira, L. & Caseiro-Alves, F. (2005). Tuberculosis of the chest. *European Journal of Radiology*, Vol. 55, No. 2, August 2005, pp. 158-172, doi:10.1016/j.ejrad.2005.04.014, ISSN 0720-048X

Daley, C.L. (2010). Update in tuberculosis 2009. *American Journal of Respiratory and Critical Care Medicine*, Vol. 181, No. 6, March 2010, pp. 550-555, ISSN 1073-449X

Davis, S.L., Be, N.A., Lamichhane, G., Nimmagadda, S., Pomper, M.G., Bishai, W.R. & Jain, S.K. (2009a). Bacterial thymidine kinase as a non-invasive imaging reporter for *Mycobacterium tuberculosis* in live animals. *PLoS One,* Vol.4, No.7, July 2009, e6297, ISSN 1932-6203

Davis, S.L., Nuermberger, E.L., Um, P.K., Vidal, C., Jedynak, B., Pomper, M.G., Bishai, W.R. & Jain, S.K. (2009b). Noninvasive pulmonary [18F]-2-fluoro-deoxy-D-glucose positron emission tomography correlates with bactericidal activity of tuberculosis drug treatment. *Antimicrobial Agents and Chemotherapy,* Vol.53, No.11, November 2009, pp. 4879-4884, ISSN 1098-6596

Dharmadhikari, A.S. & Nardell, E.A. (2008). What animal models teach humans about tuberculosis. *American Journal of Respiratory Cell and Molecular Biology*, Vol.39, No. 5, November 2008, pp. 503-508, ISSN 1535-4989

Elkington, P., Shiomi, T., Breen, R., Nuttall, R.K., Ugarte-Gil, C.A., Walker, N.F., Saraiva, L., Pedersen, B., Mauri, F., Lipman, M., Edwards, D.R., Robertson, B.D., D'Armiento, J. & Friedland, J.S. (2011). MMP-1 drives immunopathology in human tuberculosis and transgenic mice. *Journal of Clinical Investigation*, Vol. 121, No. 5, May 2011, pp. 1827-1833, ISSN 00219738

Filippi, M. & Rocca, M.A. (2011). MR imaging of multiple sclerosis. *Radiology*, Vol. 259, No. 3, June 2011, pp. 659-681, ISSN 0033-8419

Flynn, J.L. (2006). Lessons from experimental *Mycobacterium tuberculosis* infections. *Microbes and Infection*, Vol. 8, No. 4, April 2006, pp. 1179-1188, ISSN 1286-4579

Goldenberg, D.M., Chatal, J.F., Barbet, J., Boerman, O. & Sharkey, R.M. (2007). Cancer imaging and therapy with bispecific antibody pretargeting. *Update on Cancer Therapeutics*, Vol. 2, No. 1, March 2007, pp. 19-31, ISSN 1872-115X

Geraldes, C.F. & Laurent, S. (2009). Classification and basic properties of contrast agents for magnetic resonance imaging. *Contrast Media & Molecular Imaging*, Vol. 4, No. 1, January-February 2009, pp. 1-23, DOI: 10.1002/cmmi.265, ISSN 1555-4317

Gupta, U.D. & Katoch, V.M. (2005) Animal models of tuberculosis. *Tuberculosis (Edinburgh),* Vol. 85, No. 5-6, September-November 2005, pp. 277-293, ISSN 1472-9792

Hainfeld, J.F., Slatkin, D.N., Focella, T.M. & Smilowitz, H.M. (2006). Gold nanoparticles: a new X-ray contrast agent. *British Journal of Radiology*, Vol. 79, No. 939, March 2006, pp. 248-253, ISSN 0007-1285

Heuts, F., Carow, B., Wigzell, H. & Rottenberg, M.E. (2009). Use of non-invasive bioluminescent imaging to assess mycobacterial dissemination in mice, treatment with bactericidal drugs and protective immunity. *Microbes and Infection,* Vol. 11, No. 14-15, December 2009, pp. 1114-1121, ISSN 1286-4579

Hickey, M.J., Arain, T.M., Shawar, R.M., Humble, D.J., Langhorne, M.H., Morgenroth, J.N. & Stover, C.K. (1996). Luciferase in vivo expression technology: use of recombinant mycobacterial reporter strains to evaluate antimycobacterial activity in mice. *Antimicrobial Agents and Chemotherapy,* Vol. 40, No. 2, February 1996, pp. 400-407, ISSN 1098-6596

Hofmeyr, A., Lau, W.F. & Slavin, M.A. 2007. *Mycobacterium tuberculosis* infection in patients with cancer, the role of 18-fluorodeoxyglucose positron emission tomography for diagnosis and monitoring treatment response. *Tuberculosis (Edinburgh)*, Vol. 87, No. 5, September 2007, pp. 459-463, ISSN 1472-9792

Horky, L.L. & Treves, S.T. (2011). PET and SPECT in brain tumors and epilepsy. *Neurosurgery Clinics of North America*, Vol. 22, No. 2, April 2011, pp. 169-184, ISSN 1042-3680

Hsiung, P.L., Hardy, J., Friedland, S., Soetikno, R., Du, C.B., Wu, A.P., Sahbaie, P., Crawford, J.M., Lowe, A.W., Contag, C.H. & Wang, T.D. (2008). Detection of colonic dysplasia in vivo using a targeted heptapeptide and confocal microendoscopy. *Nature Medicine*, Vol. 14, No. 4, April 2008, pp. 454-458, 1078-8956

Kao, C.H., Wang, S.J. & Liu, T.J. (1994). The use of technetium-99m-rnethoxyisobutylisonitrile breast scintigraphy to evaluate palpable breast masses.

European Journal of Nuclear Medicine, Vol. 2, No. 5, May 1994, pp. 432–436, ISSN 1619-7089

Kong, Y., Subbian, S., Cirillo, S.L. & Cirillo, J.D. (2009). Application of optical imaging to study of extrapulmonary spread by tuberculosis. *Tuberculosis (Edinburgh),* Vol. 89, Suppl. 1, December 2009, pp. S15-S17, ISSN 1472-9792

Kong, Y., Yao, H., Ren, H., Subbian, S., Cirillo, S.L., Sacchettini, J.C., Rao, J. & Cirillo, J.D. (2010). Imaging tuberculosis with endogenous beta-lactamase reporter enzyme fluorescence in live mice. *Proceedings of the National Academy of Sciences of the United States of America*, Vol. 107, No. 27, July 2010, pp. 12239-12244, ISSN 1091-6490

Kraft, S. L.; Dailey, D.; Kovach, M.; Stasiak, K. L.; Bennett, J.; McFarland, C. T.; McMurray, D. N., Izzo, A. A.; Orme, I. M. & Basaraba, R. J. (2004) Magnetic resonance imaging of pulmonary lesions in guinea pigs infected with *Mycobacterium tuberculosis*. *Infection and Immunity,* Vol.72, No.10, pp. 5963–5971, ISSN 1098-5522

Kwan, C.K. & Ernst, J.D. (2011). HIV and tuberculosis: a deadly human syndemic. *Clinical Microbiology Reviews*, Vol. 24, No. 2, April 2011, pp. 351-376. ISSN 0893-8512

Leung, A.N. (1999). Pulmonary tuberculosis: the essentials. *Radiology*, Vol. 210, No. 2, February 1999, pp. 307-322, ISSN 0033-8419

Lewinsohn, D.M., Tydeman, I.S., Frieder, M., Grotzke, J.E., Lines, R.A., Ahmed, S., Prongay, K.D., Primack, S.L., Colgin, L.M., Lewis, A.D. & Lewinsohn, D.A. (2006) High resolution radiographic and fine immunologic definition of TB disease progression in the rhesus macaque. *Microbes and Infection,* Vol.8, No.11, pp. 2587-2598, ISSN 1286-4579

Li, Y.J., Zhang, Y., Gao, S. & Bai, R.J. (2008). Systemic disseminated tuberculosis mimicking malignancy on F-18 FDG PET-CT. *Clinical Nuclear Medicine*, Vol. 33, No. 1, January 2008, pp. 49-51, ISSN 0363-9762

Lin, P.L., Carney, J., Tomko, J.A., Frye, L.J., Coleman, T., Scanga, C.A., Lopresti, B.J., Mountz, J.M., Klein, E., Barry, C.E. & Flynn, J.L. (2009). Using PET/CT imaging to monitor tuberculosis progression and its response to chemotherapy in experimentally infected non-human primates. *World Molecular Imaging Congress,* Presentation number 0158, Montreal, Canada, September 2009

Liu, S.F., Liu, J.W., Lin, M.C., Lee, C.H., Huang, H.H. & Lai, Y.F. (2007). Monitoring treatment responses in patients with pulmonary TB using serial lung gallium-67 scintigraphy. *American Journal of Roentgenology*, Vol. 188, No. 5, May 2007, pp. 403–408, ISSN 0361-803X

Massoud, T.F. & Gambhir, S.S. (2003). Molecular imaging in living subjects: seeing fundamental biological processes in a new light. *Genes and Development*, Vol. 17, No. 5, March 2003, pp. 545-580, ISSN 0890-9369

Matsuura, E., Umehara, F., Hashiguchi, T., Fujimoto, N., Okada, Y. & Osame, M. (2000). Marked increase of matrix metalloproteinase 9 in cerebrospinal fluid of patients with fungal or tuberculous meningoencephalitis. *Journal of the Neurological Sciences*, Vol. 173, No. 1, February 2000, pp. 45-52, ISSN 0022-510X

McAdams, H.P., Erasmus, J. & Winter, J.A. (1995). Radiologic manifestations of pulmonary tuberculosis. *Radiologic Clinics of North America*, Vol. 33, No. 4, July 1995, pp. 655-678, ISSN 0033-8389

McClennan, B.L. (1994). Adverse reactions to iodinated contrast media. Recognition and response. *Investigative Radiology*, Vol. 29, Suppl. 1, May 1994, pp.S46-50, ISSN 0020-9996

Ntziachristos, V. (2006). Fluorescence molecular imaging. *Annual Review of Biomedical Engineering*, Vol. 8, August 2006, pp. 1-33, ISSN 1523-9829

Önsel, C., Sönmezoglu, K., Camsari, G., Atay, S., Cetin, S., Erdil, Y.T., Uslu, I., Uzun, A., Kanmaz, B. & Sayman, H.B. (1996). Technetium-99m-MIBI scintigraphy in pulmonary tuberculosis. *Journal of Nuclear Medicine*, Vol. 37, No. 2, February 1996, pp. 233–238, ISSN 0161-5505

Ordway, D.J., Shanley, C.A., Caraway, M.L., Orme, E.A., Bucy, D.S., Hascall-Dove, L., Henao-Tamayo, M., Harton, M.R., Shang, S., Ackart, D. Kraft, S.L., Lenaerts, A.J., Basaraba, R.J. & Orme, I.M. (2010). Evaluation of standard chemotherapy in the guinea pig model of tuberculosis. *Antimicrobial Agents and Chemotherapy,* Vol. 54, No. 5, May 2010, pp. 1820-1833, ISSN 1098-6596

Pirko, I., Johnson, A., Ciric, B., Gamez, J., Macura, S.I., Pease, L.R. & Rodriguez, M. (2004). In vivo magnetic resonance imaging of immune cells in the central nervous system with superparamagnetic antibodies. *FASEB Journal* (the official publication of the Federation of American Societies for Experimental Biology), Vol. 18, No. 1, January 2004, pp. 179-182, ISSN 0892-6638

Pysz, M.A., Gambhir, S.S. & Willmann, J.K. (2010). Molecular imaging: current status and emerging strategies. *Clinical Radiology*, Vol. 65, No. 7, July 2010, pp. 500-516, ISSN 0009-9260

Rabin, O., Manuel Perez, J., Grimm, J., Wojtkiewicz, G. & Weissleder, R. (2006). An X-ray computed tomography imaging agent based on long-circulating bismuth sulphide nanoparticles. *Nature Materials*, Vol. 5, No. 2, February 2006, pp. 118-122, ISSN 1476-1122

Sandhu, G.S., Solorio, L., Broome, A.M., Salem, N., Kolthammer, J., Shah, T., Flask, C. & Duerk, J.L. (2010). Whole animal imaging. *Wiley Interdisciplinary Reviews. Systems Biology and Medicine*, Vol. 2, No. 4, July-August 2010, pp. 398-421, ISSN 1939-005X

Sharpe, S.A., Eschelbach, E., Basaraba, R.J., Gleeson, F., Hall, G.A., McIntyre, A., Williams, A., Kraft, S.L., Clark, S., Gooch, K., Hatch, G., Orme, I.M., Marsh, P.D. & Dennis, M.J. (2009). Determination of lesion volume by MRI and stereology in a macaque model of tuberculosis. *Tuberculosis (Edinburgh),* Vol. 89, No. 6, November 2009, pp. 405-416, ISSN 1472-9792

Sharpe, S.A., McShane, H., Dennis, M.J., Basaraba, R.J., Gleeson, F., Hall, G., McIntyre, A., Gooch, K., Clark, S., Beveridge, N.E., Nuth, E., White, A., Marriott, A., Dowall, S., Hill, A.V., Williams, A. & Marsh, P.D. (2010). Establishment of an aerosol challenge model of tuberculosis in rhesus macaques and an evaluation of endpoints for vaccine testing. *Clinical and Vaccine Immunology,* Vol.17, No.8, August 2010, pp. 1170-1182, ISSN 1556-679X

Signore, A. & Glaudemans, A.W. (2011). The molecular imaging approach to image infections and inflammation by nuclear medicine techniques. *Annals of Nuclear Medicine*, DOI: 10.1007/s12149-011-0521-z, Epub ahead of print: Aug 12, ISSN 0914-7187

Singh, S.P. & Nath, H. (1994). Early radiology of pulmonary tuberculosis. *American Journal of Roentgenology*, Vol. 162, No. 4, April 1994, pp. 846, ISSN 0361-803X

Snewin, V.A., Gares, M.P., Gaora, P.O., Hasan, Z., Brown, I.N. & Young, D.B. (1999). Assessment of immunity to mycobacterial infection with luciferase reporter constructs. *Infection and Immunity,* Vol. 67, No. 9, September 1999, pp. 4586-4593, ISSN 1098-5522

Stefanescu, C., Rusu, V., Boisteanu, D., Azoicai, D., Costin, M., Oleniuc, D., Hurjui, M. & Sattish, P. (2006). 99mTc isonitrils biophysical aspects in pulmonary tuberculosis. Part I. In vivo evaluation of 99mTc MIBI and 99mTc tetrofosmin biophysical localization mechanisms. *Revista Medico Chirurgicala a Societatii de Medici si Naturalisti din Iasi*, Vol. 110, No. 4, October-December 2006, pp. 944–949, ISSN 0300-8738

Stefanescu, C., Rusu, V., Azoici, D. & Hurjui, I. (2007). 99mTc isonitrils biophysical aspects in pulmonary tuberculosis. Part II. In vitro evaluation of 99mTc MIBI cellular uptake mechanism. *Revista Medico Chirurgicala a Societatii de Medici si Naturalisti din Iasi*, Vol. 111, No. 1, January-March 2007, pp. 210–215, ISSN 0300-8738

Sugawara, I., Mizuno, S., Tatsumi, T. & Taniyama, T. (2006) Imaging of pulmonary granulomas using a photon imager. *Japanese Journal of Infectious Diseases,* Vol. 59, No. 5, October 2006, pp. 332-333, ISSN 1344-6304

Tarantal, A.F., Lee, C.C., Jimenez, D.F. & Cherry, S.R. (2006). Fetal gene transfer using lentiviral vectors: in vivo detection of gene expression by microPET and optical imaging in fetal and infant monkeys. *Human Gene Therapy*, Vol. 17, No. 12, December 2006, pp. 1254-1261, ISSN 1043-0342

Taschereau, R., Silverman, R.W. & Chatzijoannou, A.F. (2010). Dual-energy attenuation coefficient decomposition with differential filtration and application to a micro-CT scanner. *Physics in Medicine and Biology*, Vol. 55, No. 4, February 2010, pp. 1141-1155, ISSN 0031-9155

Troy, T., Jekic-McMullen, D., Sambucetti, L. & Rice, B. (2004). Quantitative comparison of the sensitivity of detection of fluorescent and bioluminescent reporters in animal models. *Molecular Imaging*, Vol. 3, No. 1, January 2004, pp. 9-23, ISSN 1535-3508

Wiles, S., Crepin, V.F., Childs, G., Frankel, G. & Kerton, A. (2007). Use of biophotonic imaging as a training aid for administration of substances in laboratory rodents. *Laboratory Animals*, Vol. 41, No. 3, July 2007, pp. 321-328, ISSN 0023-6772

Vanhagen, P.M., Krenning, E.P., Reubi, J.C., Kwekkeboom, D.J., Bakker, W.H., Mulder, A.H., Laissue, I., Hoogstede, H.C. & Lamberts, S.W. (1994). Somatostatin analogue scintigraphy in granulomatous diseases. *European Journal of Nuclear Medicine*, Vol. 21, No. 6, June 1994, pp. 497–502, ISSN 1619-7089

World Health Organisation. (2010). Global tuberculosis control 2010: WHO Press, 2010

Yang, A., Xue, J., Li, X., Yu, Y., Deng, H., Hu, G., Meng, X. & Li, J. (2007). Experimental and clinical observations of 99mTc-MIBI uptake correlate with P-glycoprotein expression in lung cancer. *Nuclear Medicine Communications*, Vol. 28, No. 9, September 2007, pp. 696–703, ISSN 0143-3636

Yang, C.M., Hsu, C.H., Lee, C.M. & Wang, F.C. (2003). Intense uptake of [F-18]-fluoro-2 deoxy-D-glucose in active pulmonary tuberculosis. *Annals of Nuclear Medicine*, Vol. 17, No. 5, July 2003, pp. 407-410, ISSN 0914-7187

Zonios, G., Bykowski, J. & Kollias, N. (2001). Skin melanin, hemoglobin, and light scattering properties can be quantitatively assessed in vivo using diffuse reflectance spectroscopy. *Journal of Investigative Dermatology*, Vol. 117, No. 6, December 2001, pp. 1452-1457, ISSN 0022-202X

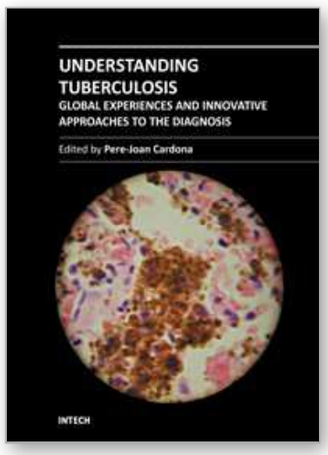

Understanding Tuberculosis - Global Experiences and Innovative Approaches to the Diagnosis

Edited by Dr. Pere-Joan Cardona

ISBN 978-953-307-938-7
Hard cover, 552 pages
Publisher InTech
Published online 15, February, 2012
Published in print edition February, 2012

Mycobacterium tuberculosis is a disease that is transmitted through aerosol. This is the reason why it is estimated that a third of humankind is already infected by Mycobacterium tuberculosis. The vast majority of the infected do not know about their status. Mycobacterium tuberculosis is a silent pathogen, causing no symptomatology at all during the infection. In addition, infected people cannot cause further infections. Unfortunately, an estimated 10 per cent of the infected population has the probability to develop the disease, making it very difficult to eradicate. Once in this stage, the bacilli can be transmitted to other persons and the development of clinical symptoms is very progressive. Therefore the diagnosis, especially the discrimination between infection and disease, is a real challenge. In this book, we present the experience of worldwide specialists on the diagnosis, along with its lights and shadows.

InTech Europe
University Campus STeP Ri
Slavka Krautzeka 83/A
51000 Rijeka, Croatia
Phone: +385 (51) 770 447
Fax: +385 (51) 686 166
www.intechopen.com

InTech China
Unit 405, Office Block, Hotel Equatorial Shanghai
No.65, Yan An Road (West), Shanghai, 200040, China
中国上海市延安西路65号上海国际贵都大饭店办公楼405单元
Phone: +86-21-62489820
Fax: +86-21-62489821

IntechOpen